Open access • Journal Article • DOI:10.1029/1999JA000244

Global Positioning System measurements of the ionospheric zonal apparent velocity at Cachoeira Paulista in Brazil — Source link

Hyosub Kil, Paul M. Kintner, Eurico R. de Paula, Ivan J. Kantor

Published on: 01 Mar 2000 - Journal of Geophysical Research (John Wiley & Sons, Ltd)

Topics: TEC, Total electron content and Earth's magnetic field

JOURNAL OF GEOPHYSICAL RESEARCH, VOL. 105, NO. A3, PAGES 5317-5327, MARCH 1, 2000

Global Positioning System measurements of the ionospheric zonal apparent velocity at Cachoeira Paulista in Brazil

Hyosub Kil and Paul M. Kintner

School of Electrical Engineering, Cornell University, Ithaca, New York

Eurico R. de Paula and Ivan J. Kantor

Instituto Nacional de Pesquisas Espaciais-DAE, São José dos Campos, São Paulo, Brazil

Abstract. Ionospheric irregularities and their zonal apparent drift were studied using Global Positioning System (GPS) measurements at Cachoeira Paulista (22.41°S, 45.00°W, −26° dip angle) in Brazil during November 6-19, 1998. Radio scintillations at the GPS L1 frequency (1.575 GHz) were monitored using four GPS receivers spaced geomagnetically east-west and north-south. Total electron content (TEC) was measured through the ionospheric advance of the GPS L1 and L2 (1.227 GHz) phases. Strong amplitude scintillations coincided with TEC fluctuations associated with spread F bubbles elongated along the magnetic field. Movement of the Fresnel-scale (400 m) ionospheric irregularity layers caused the scintillation to drift, and their zonal apparent drift velocities were measured using a cross-correlation technique. Our measurements show that the apparent eastward velocity varies from 200 m/s to 150 m/s at 2000 LT, and then it decreases to 100-50 m/s at midnight. On a magnetically disturbed day, reversal of the zonal apparent drift was observed just after midnight, and the apparent westward velocities observed at early in the morning showed large variations with location in the sky. From the receivers spaced in the geomagnetic north-south direction we measured near-zero time shifts, from which we conclude that the correlation length of several-hundred-meter-scale irregularities is much larger than 70-m separation between the north and south receivers.

1. Introduction

The study of ionospheric plasma drifts is of fundamental importance in understanding the F region dynamo and the equatorial spread F phenomenon in the low-latitude region. The plasma drifts perpendicular to the magnetic field result from the polarization electric fields generated by the neutral wind-driven currents in the ionosphere [*Heelis et al.*, 1974; *Richmond et al.*, 1976; *Farley et al.*, 1986]. During daytime the E region electric fields produced by the tidal winds control the plasma drift in the F region. After sunset, the E region conductivity is much reduced, and the plasma drifts eastward under the control of the F region dynamo electric fields.

The most extensive observations of the zonal drift velocity at the magnetic equator have been made from incoherent scatter radar station at Jicamarca in Peru [*Woodman*, 1972; *Fejer*, 1981]. The drift pattern shows a typical diurnal cycle consisting of westward drifts with 50 m/s during the day and eastward drifts up to 130 m/s in the evening. The evening reversal time and the magnitude of the daytime drift velocity are nearly independent of solar flux and magnetic activity, but the morning reversal time and the magnitude of the nighttime velocity are variable with their change [*Fejer et al.*, 1991]. The daytime westward drift velocity is smaller than the nighttime eastward velocity, which leads to a net superrotation of the equatorial ionosphere. While the observations at Jicamarca give information of the zonal drift velocity near the F peak height at the magnetic equator, the global distributions at low-dip latitudes were studied with the DE-2 satellite measurements of the vertical electric field [*Aggson et al.*, 1987; *Maynard et al.*, 1988; *Coley and Heelis*, 1989]. In the presence of spread F during the night the local zonal drift velocities were observed on the ground from the time lags of radio scintillations [*Basu et al.*, 1980, 1991, 1996; *Valladares et al.*, 1996] and total electron content (TEC) depletions [*Abdu et al.*, 1985a, b], and from the movement of the airglow images [*Mendillo and Baumgardner*, 1982; *Abdu et al.*, 1987; *Rohrbaugh et al.*, 1989;

Paper number 1999JA000244
0148-0227/00/1999JA000244$09.00

Sobral and Abdu, 1990, 1991; *Tinsley et al.,* 1997]. All the observations on the ground and on board satellite agree with the canonical diurnal zonal drift pattern observed at Jicamarca. However, local and temporal variations of the magnitude and reversal time of the zonal velocity were also observed. For better statistics in the global distributions of the plasma drifts, further continuous observations in worldwide locations are still required.

The establishment of Global Positioning System (GPS) has provided a new set of tools for the research of ionospheric irregularities and their effect on the radio wave propagation [*Aarons et al.,* 1996; *Kelley et al.,* 1996; *Beach et al.,* 1997; *Musman et al.,* 1997]. It provides a global and continuous signal and data source which can be accessed through several governmental and private information services [*Hofmann-Wellenhof et al.,* 1994] or can be collected directly by user developed GPS receivers. GPS receivers developed at Cornell University are distributed on several places in the South America and are continuing data collection regularly and on campaign basis since 1995. In 1998, a GPS campaign was conducted during November at Cachoeira Paulista (22.41°S, 45.00°W, −26° dip angle) in Brazil, near the crest of the equatorial anomaly during the spread F season.

The purpose of this paper is to verify that the zonal drift velocity can adequately be measured with Cornell GPS receivers as well as to report the zonal apparent drift velocity in this region. A brief description of the Cornell GPS receiver and campaign is given. We present 8 days of zonal apparent velocity measurements and discuss a vertical shear of the zonal plasma flow. Finally, summary and future work are given.

2. Campaign Descriptions

The space physics group at Cornell University developed a GPS receiver, named SCINTMON, for the purpose of monitoring ionospheric scintillation. It is based on a GEC Plessey GPS development system but modified for a fast logging of the signal strength (50 samples/s rate) of the GPS L1 frequency (1.575 GHz) [*Beach,* 1998]. Cornell University GPS campaign collaborated with Instituto Nacional de Pesquisas Espaciais (INPE) and was conducted at Cachoeira Paulista in Brazil during November 6-19, 1998. By deploying four SCINTMONs, three of them geomagnetically east-west and one of them geomagnetically north, we aimed at measuring the ionospheric zonal drift velocity and investigating the correlation length of the Fresnel scale irregularities in the field direction. The dual-frequency receiver, Allen Osborne ICS-4000Z (AOA), was operated to measure a TEC with a maximum sampling frequency 1 Hz. Figure 1 shows the receiver locations with station identifications in the boxes. Stations W, S and E are aligned magnetically east-west with spacing 79 m for W-S and 50 m for S-E. Station N is located 70 m geomagnetically north from the station S. The dual frequency receiver (AOA) was placed near station N. The magnetic field line is slanted 19° westward from the true north. Our observations were limited to night times during 1800-0600 LT.

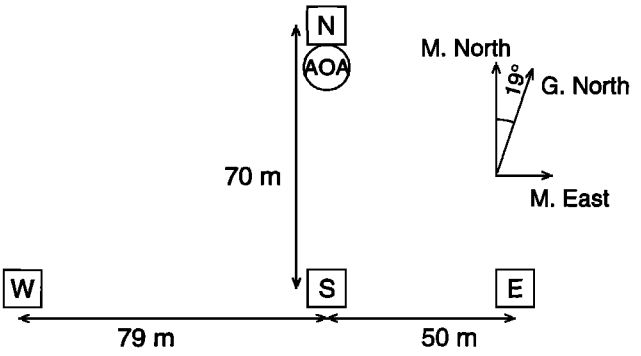

Figure 1. Deployment of Global Positioning System (GPS) receivers. Three receivers (W, S and E) are spaced geomagnetically west-east and one receiver (N) is spaced geomagnetically north. The dual-frequency receiver (AOA) is placed near station N.

3. Observations and Discussion

Electron density irregularities in the F region are primarily responsible for the radio scintillation and TEC fluctuations. Since the ionospheric irregularities in the low-latitude region are often associated with plasma-depleted flux tubes, the TEC fluctuations appear as TEC depletions relative to the background. Measurements of scintillation and TEC from satellites 14 (PRN 14) and 15 (PRN 15) on the night of November 10-11 are presented in Figure 2a. The signal powers in the top plots are sampled every 1 s. The S_4 indices on the middle plots are defined as the standard deviation of the signal powers divided by their mean and calculated every 1 min using 3000 points of the signal power measurements. The relative TECs on the bottom plots are calculated from the ionospheric advance of the GPS L1 and L2 phases. The TEC unit is given by TECU ($10^{16}/m^2$). The satellite paths are shown on the azimuth-elevation coordinates in Figure 2b. The widths of the paths are made proportional to the magnitude of S_4 index. The dashed line slanted 19° westward indicates the direction of the geomagnetic field. Strong amplitude scintillations were observed around 2200-2300 LT from both of satellites, and the paths of the satellites at that time range are shaded black in the plot. As the elevation increased, the signal power increased owing to the decrease of the distance that the radio wave traveled, whereas the TEC decreased because of the decrease of integration path length. Strong scintillations and, consequently, large S_4 indices were observed with large TEC depletions and fluctuations. Very similar TEC structures were observed at 2200-2300 LT when the two satellites were aligned parallel to the magnetic

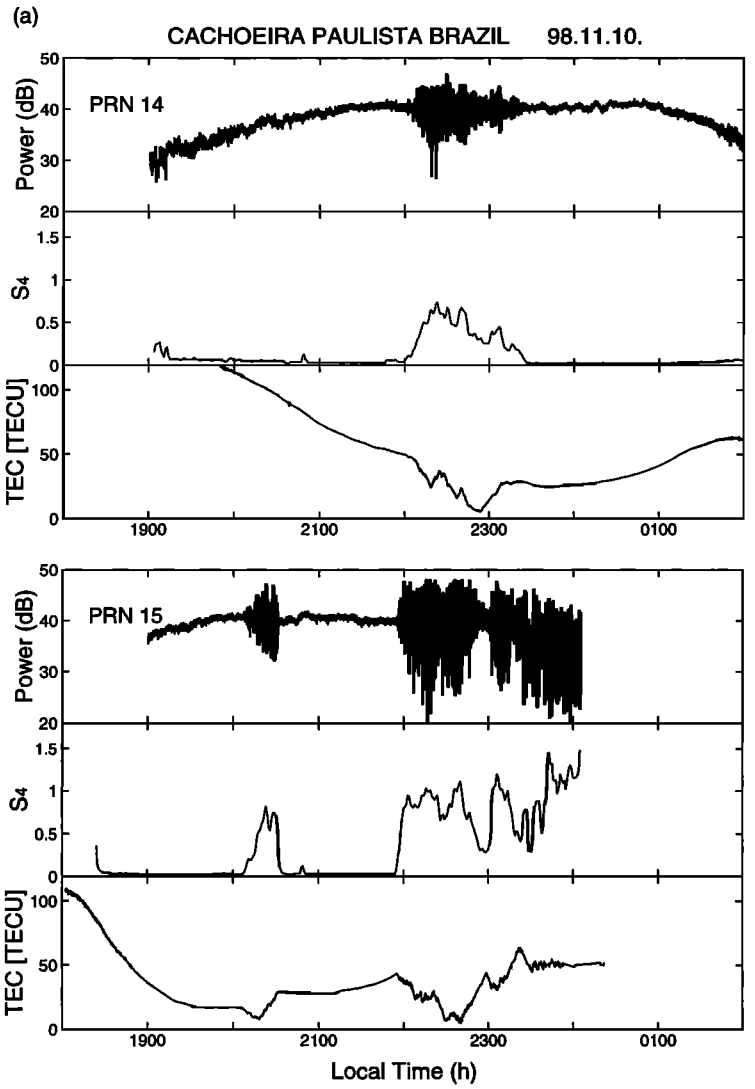

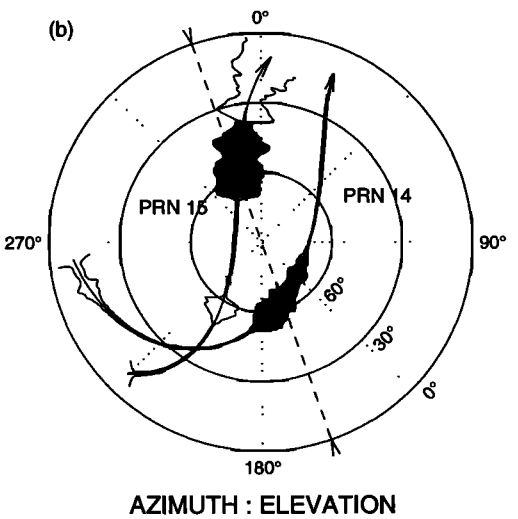

Figure 2. Scintillation and total electron content (TEC) measurements from (a) satellites 14 (PRN 14) and 15 (PRN 15) and (b) satellite paths on the azimuth-elevation coordinates. The path width is made proportional to the magnitude of S_4 index. Large TEC depletions are observed around 2200-2300 LT from the two satellites, and those paths are shaded black. The dashed line indicates the direction of the magnetic field.

field north-south direction. They are believed to have been caused by a drifting patch of plasma density depletions which was extended along the magnetic field.

Scintillation drift is a well-known technique to measure the ionospheric zonal drift velocity [*Vacchione et al.*, 1987; *Spatz et al.*, 1988; *Basu et al.*, 1991, 1996; *Valladares et al.*, 1996]. Basically, our GPS observations employed the same measurement technique. The differences from the previous observations, which were made by use of the geostationary satellite signal, are the movement of GPS satellites and multiple observations from multiple satellites at different locations in the sky. In determining a velocity, accurate measurements of time and distance are essential. The cross-correlation offset time can be determined accurately by virtue of the high sampling rate of the receiver and by virtue of the synchronization of the measurement times with precise GPS time. On the other hand, the distance contains some ambiguities because it should be the distance that the irregularity layers move in the ionosphere rather than the distance on the ground. The distance from a receiver to a satellite is at least 20,000 km, while that from a receiver to the F peak is $<$ 1000 km and usually is $\sim$ 350 km. Therefore the distance on the ground is not so different from that in the ionosphere. In the case of geostationary satellites the subionospheric distance may not change. However, for GPS it varies as the satellites move, and we have found that the subionospheric distance is significantly reduced at low elevations ($< 40° \sim 50°$). At high elevations the subionospheric distance at 350-km altitude did not change much with elevations and appeared to be shorter $\sim$ 4% than the distance on the ground. In the following analysis we will apply this correction to a subionospheric distance and include observations made at high elevations ($> 40°$).

Signal power measurements from PRN 14 in Figure 2 are sampled from four receivers, and Figure 3a shows the variations of scintillation pattern for 2 min. The scintillation patterns are very similar, but they appear as a slight time shift between receivers. The ionospheric irregularities drifting eastward relative to the satellite will meet the receiver W first and then S and E, and the lag time increases with distance between the antennas. Note that there is almost no time lag between S and N, receivers in the north-south direction. We measured the time lag quantitatively using the cross-correlation technique. The cross-correlation function $C(\tau)$ between the two signal intensities S_1 and S_2 is given by

$$C(\tau) = \frac{\sum_k S_1(t_k)\, S_2(\tau - t_k)}{\sqrt{\sum_k {S_1}^2(t_k)\ \sum_k {S_2}^2(t_k)}}. \qquad (1)$$

Figure 3b presents the cross correlations and offset numbers between the scintillation patterns. In these plots the cross-correlation offsets are calculated referenced to the west and south sites. So the positive offset means that the scintillation pattern is moving either eastward or northward depending on the receiver alignment, one unit of the offset corresponding to 0.02 s. The offset between W-E is one point less than the sum of the offsets between W-S and S-E, which shows the self-consistency of our measurements.

Apparent plasma drift velocity can be inferred by measuring the maximum correlation time. It corresponds to the mean bulk plasma drift velocity under the assumption of frozen-in irregularity structure during the correlation time. However, owing to the random fluctuations of the electron density the apparent velocity v' is given by the Briggs' full correlation method

$$v' = v_o + \frac{{v_c}^2}{v_o}, \qquad (2)$$

where v_o is the mean true velocity and v_c is the characteristic random velocity [*Briggs*, 1968; *Wernik et al.*, 1983]. In this study, we measured the apparent drift velocity, ignoring the characteristic random velocity. We found that the characteristic time (the time that the autocorrelation function is equal to the peak of the cross-correlation function) was largely variable owing to the decorrelation on the cross-correlation function by noise, which caused considerable errors to the deduced true velocity. Previous observations showed that the characteristic random velocity was maximum during periods of irregularity growth and then it rapidly decreased as the night progressed [*Vacchione et al.*, 1987; *Spatz et al.*, 1988]. The characteristic random velocity observed by *Spatz et al.* [1988] using UHF signal with baseline 457.2 m showed $\sim$ 30 m/s before 2200 LT and then $<$ 10 m/s at midnight. Assuming 100 m/s of the true ionospheric drift velocity, the apparent velocity is greater than the true velocity $\sim$ 10 m/s before 2200 LT, and then the difference is reduced to 1 m/s at midnight. Therefore the apparent velocity may be approximated to the mean true velocity with errors $<$ 10 m/s. The relative apparent drift velocity v_r' of the irregularities to the satellite movement is determined using the relation $v_r' = d/(j/R)$, where d is the subionospheric distance, j is the offset number, and R is the sampling rate. In this case the apparent velocities are 92 m/s for W-S, 94 m/s for S-E, and 94 m/s for W-E. If the satellite is stationary, then the measured apparent velocities will directly be the apparent drift velocities of the ionospheric irregularities. However, the satellite east-west movement gives the same effect as the irregularity layers moving in the opposite direction to the satellite. That is, if we assume that the irregularities are stationary but the satellite is moving eastward with a velocity v_s, then the receiver on the ground will measure the movement of scintillation pattern westward with a velocity v_s. Therefore the apparent irregularity drift velocity v' on the ground is given by the relation $v' = v_r' + v_s$. By adding 50 m/s for v_s measured at 2230 LT at 350-km altitude the apparent ionospheric irregularity drift velocity is found to be 143 m/s eastward.

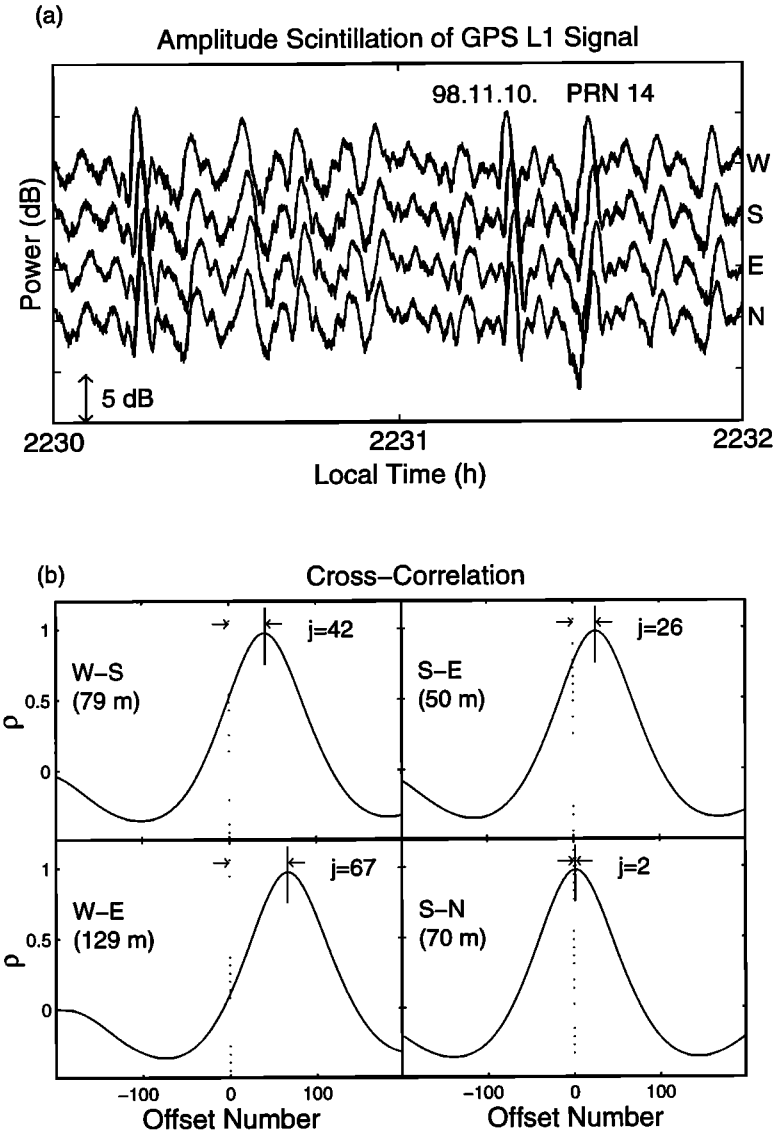

Figure 3. (a) Signal powers sampled for 2 min from four receivers and (b) their cross correlations. The offset numbers are measured from the center to the maximum correlation index, and the time shifts are calculated dividing them by the sampling rate (50 Hz).

By applying a similar method described above, we calculated the apparent drift velocity from the measurements of the two satellites shown in Figure 2. The satellite paths are shaded black during that time range in Figure 2b. Figure 4 shows the cross-correlation offset numbers in the top plots, satellite magnetic eastward velocities in the middle plots, and the inferred apparent ionospheric drift velocities in the bottom plots. We assumed the altitude of the ionospheric irregularity layer to be 350 km. The offset numbers depend on the distances between the receivers, but they consistently return very similar apparent drift velocities. The offsets between the north-south stations remain almost constant. It confirms the idea that the correlation length of Fresnel-scale ($\sim$ 400 m) irregularities along the field line is much larger than the distance between the receivers (70 m). We can estimate the size of irregularity patch that caused scintillations and TEC depletions in Figure 2. Multiplying the apparent drift velocity relative to the satellite ($\sim$ 100 m/s) by the time range of TEC depletions (2200-2320 LT), the bubble size is estimated to be 480 km.

The postmidnight spread F is known to be strongly affected by magnetic activity and is enhanced during active times [*Aarons et al.*, 1980; *Rastogi et al.*, 1981; *Batista et al.*, 1990; *Kelley and Maruyama*, 1992]. We observed weak scintillations ($S_4 < 0.3$) after midnight on November 13-14 when the Kp index was 6^0. On that night the zonal apparent velocity reversal from east to west was observed near midnight. The inferred apparent drift velocities and satellite paths on the azimuth-elevation coordinates are shown in Figure 5. Measure-

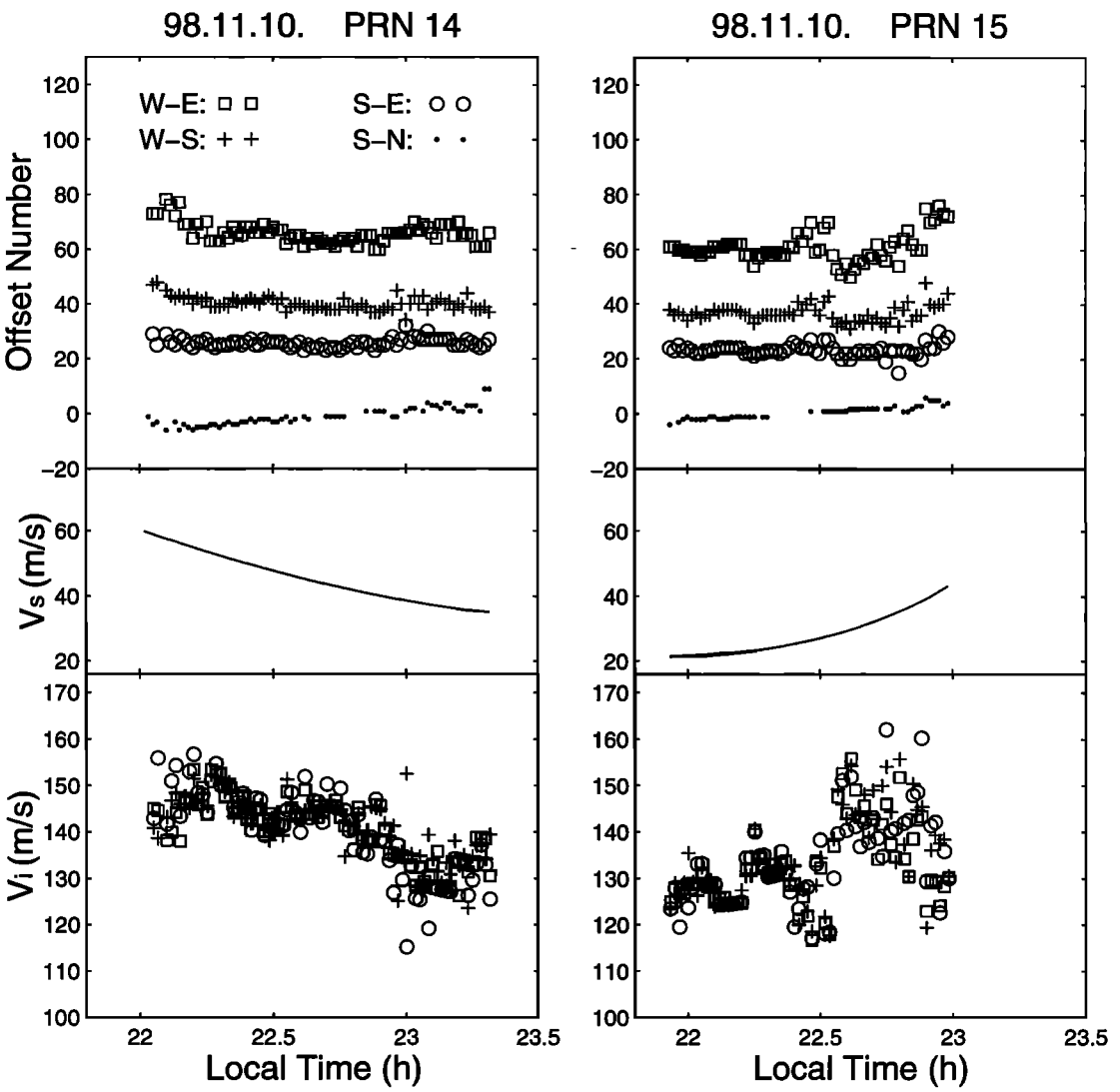

Figure 4. Zonal apparent drift velocities inferred from PRN 14 and 15. The top plots are offset numbers. The middle plots are the magnetic eastward velocity of the satellites in the ionosphere at 350-km altitude. By adding the satellite velocity to the relative velocity calculated from the time shifts the apparent ionospheric drift velocity is obtained in the bottom plots.

ments from each satellite are distinguished by different symbols. The apparent drift velocities are calculated only when the satellites are above 40° elevation, which is indicated by dotted circles. The magnitude of S_4 index designated by the width of satellite path remains near 0.2 after midnight. Similar apparent drift velocities were measured from all satellites until 0230 LT, but the apparent velocities measured from satellites 13, 18, and 27 became largely different after 0300 LT. On the path of the satellite 27 the apparent velocity fluctuated $\sim$ 100 m/s during 0400-0500 LT. The GPS observations showed both temporal and spatial variations of the apparent velocity. The zonal apparent drift pattern observed on that night conformed to the previous experiments, which showed much small eastward velocity, early reversal, and fluctuations in the presence of magnetic disturbance. [*Abdu et al.*, 1985*b*; *Basu et al.*, 1996; *Valladares et al.*, 1996]. On the magnetically disturbed night the vertical drifts of irregularities can significantly affect the zonal velocity inferred from the scintillation drift since the scintillation activity after midnight is known to be triggered by the fluctuating zonal electric fields which cause the fluctuations of the vertical velocity. Its effect may appear more significant when the satellite (such as PRN 18) is off longer distance from the magnetic meridian of the receiver. At the location of the satellite 18 around 0300 LT the apparent cross-correlation time becomes shorter in the presence of upward drift, and we measure larger westward velocity. The effect of the vertical drift on the zonal velocity is discussed later.

The daily variations of the zonal apparent velocities during the campaign period are presented in Figure 6. In this calculation, we included data of elevation > 50°

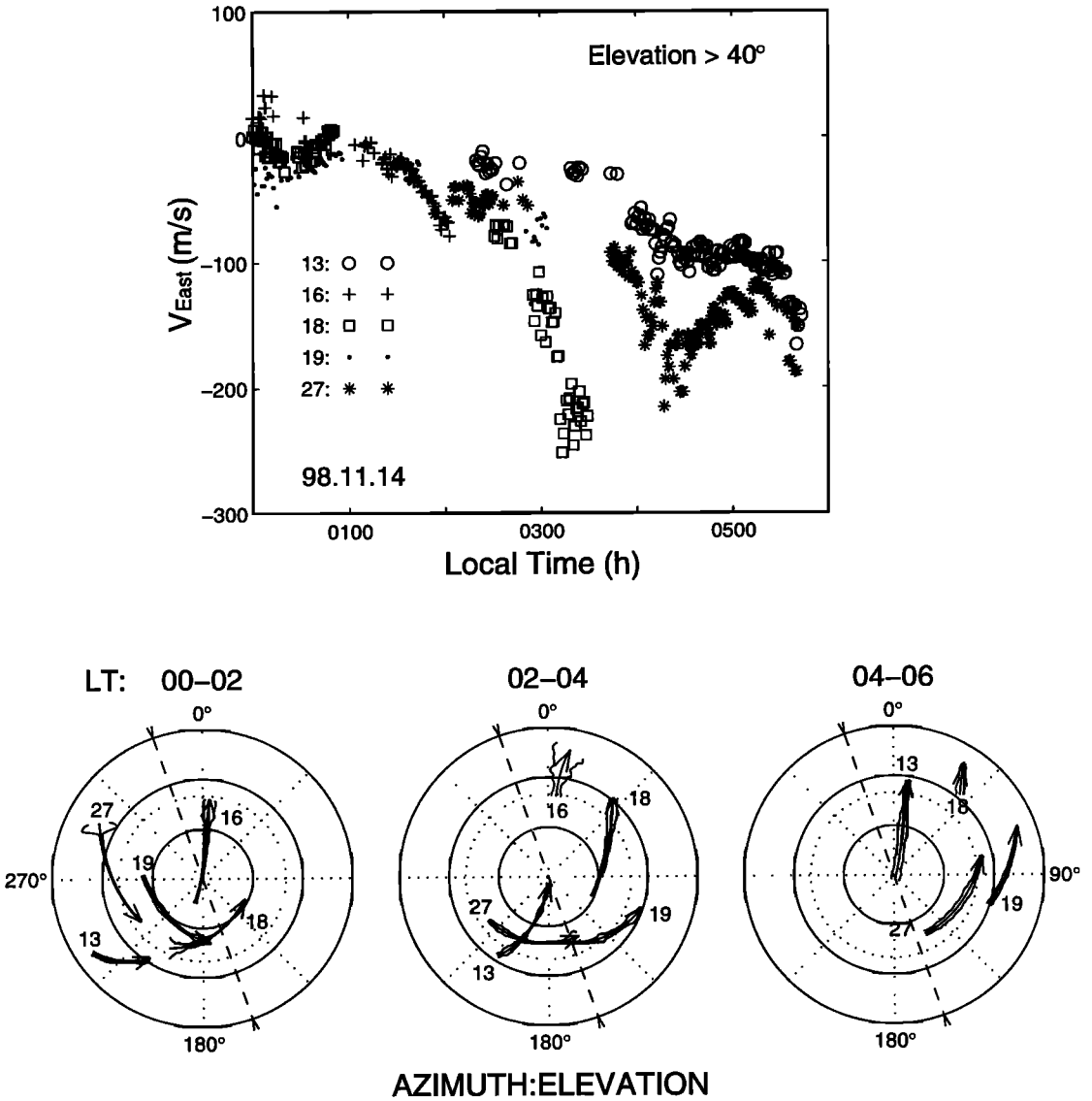

Figure 5. Zonal apparent velocities on the magnetically disturbed night and the satellite paths in the azimuth-elevation coordinates.

and S_4 index > 0.1. In most of days, except day 13, the drift velocity was missing after midnight owing to the absence of scintillation. There were day by day variations, but the results commonly showed a decrease of the apparent eastward velocity with time. The apparent velocity had a maximum value around 150-200 m/s at 2000 LT and decreased linearly to 50-100 m/s at midnight. On night 13-14 the apparent eastward velocities were a little smaller than those on the other days, and the zonal apparent velocity reversal occurred at midnight. The apparent westward velocity reached as much as 100 m/s at 0500 LT.

The comparison of the zonal velocities at different latitudes has special interest for the study of zonal plasma flow in the ionosphere. In Figure 7, we presented the average apparent drift velocities inferred from the GPS observations and the incoherent radar measurements in 1970-1971 at Jicamarca [*Fejer et al.*, 1981]. The former observations represent the zonal drift near the crest of the equatorial anomaly and the latter at the magnetic equator. In this plot we exclude data on day 13 because it behaved largely different from those made on the other days. Both set observations agree in that the drift pattern showed an increase in velocity before 2000-2100 LT following a decrease. However, the magnitude of the apparent velocity at Cachoeira Paulista was consistently greater than that at Jicamarca. We should note that the GPS measurements were made when the sunspot number was increasing rapidly after the minimum epoch while the measurements at Jicamarca were made close to the epoch of higher solar activity. We also have to consider the different ionospheric conditions when the observations were made. That is, the apparent velocities at Cachoeira Paulista were mea-

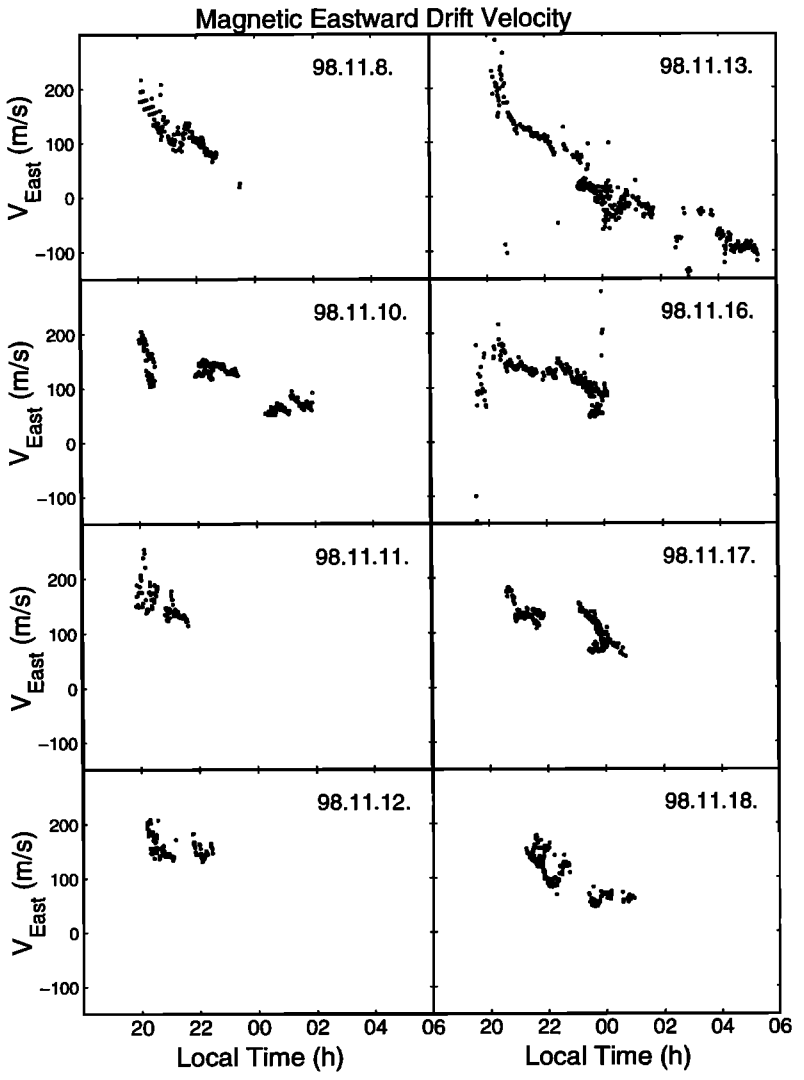

Figure 6. Measurements of the zonal apparent drift velocity during the campaign period.

sured in the presence of spread F, whereas those at Jicamarca were made in the absence of spread F. *Valladares et al.* [1996] obtained reasonable zonal velocities at Ancon in Peru, measuring the scintillation drifts of the geostationary satellite signal, but their results were consistently greater than the observations made at Jicamarca. During spread F time the ionosphere is lifted to higher altitudes through postsunset enhancement of the upward velocity. Then, the zonal wind velocity is increased owing to the reduced ion drag, which in turn, enhances the zonal plasma drift velocity. The magnitudes of the apparent velocities inferred from the GPS measurements are by $\sim$ 50 m/s smaller than those deduced from the TEC measurements [*Abdu et al.*, 1985a, b], although both observations were made at the same location. On average, our and previous observations at Cachoeira Paulista show that the zonal apparent velocity near the equatorial anomaly (in the Brazilian sector) is greater than the true velocity at the magnetic equator (in Peru), especially at early evening hours.

Because of the extended nature of the irregularities along the magnetic field the latitudinal difference of the zonal velocity is understood as an indication of vertical shear of the bulk plasma flow in the equatorial plane. The vertical shear of the ionospheric zonal drifts were reported in many observations [*Woodman and La Hoz*, 1976; *Fejer*, 1981; *Kudeki et al.*, 1981; *Aggson et al.*, 1987; *Coley and Heelis*, 1989; *Basu et al.*, 1991] and was reproduced by the model calculations [*Zalesak et al.*, 1982; *Anderson and Mendillo*, 1983]. The zonal velocity is expressed as a product of the zonal neutral wind velocity and the Perdersen conductivity integrated along the magnetic field line [*Anderson and Mendillo*, 1983]. They showed that the integrated vertical electric field increased rapidly up to around 500 km and then slowly decreased when they assumed a decrease of the zonal neutral wind velocity with an increase of the latitude in their model calculation. This drift morphology agrees with the DE-2 satellite observations which showed the maximum drift velocities around $\pm 8°$ dip latitudes [*Ag-*

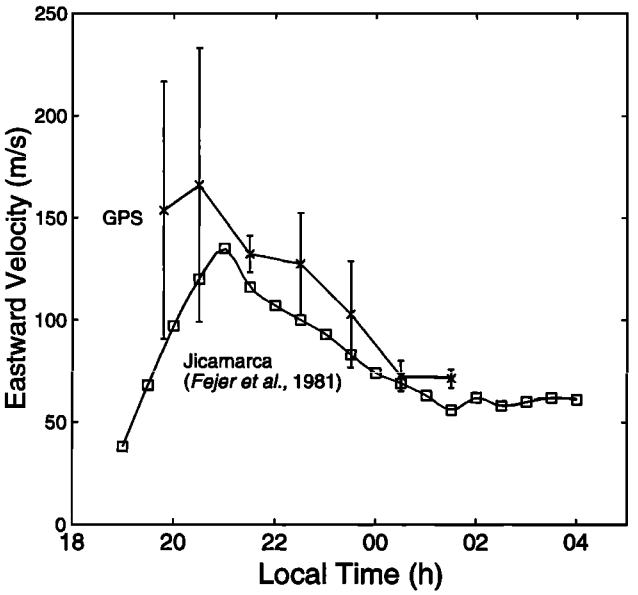

Figure 7. Average zonal apparent drift velocities inferred from the GPS measurements. For comparison we plotted together observations at Jicamarca [*Fejer et al.*, 1981].

gson et al., 1987]. The ionosphere of 350-km altitude at the latitude of Cachoeira Paulista is mapped to 700-km altitude at the magnetic equator, and therefore the zonal velocity falls to the slowly decreasing phase following the model calculation and DE-2 satellite observations. The magnitude of zonal velocity observed at 3.7°S magnetic latitude in Peru [*Basu et al.*, 1991] is similar to that at Cachoeira Paulista. Their observations may fall to the rapidly increasing phase below the peak velocity in the model calculation. These observations at off magnetic latitudes can be regarded as an implication of a possible minimum zonal velocity at the magnetic equator during nighttime. However, as discussed above, the zonal velocity is variable with ionospheric conditions, and we have to be careful in the comparison of observations made at different time periods. Simultaneous measurements for a long-term period are required at least at the equatorial anomaly and between the magnetic equator and anomaly to understand the latitudinal distributions of the zonal drifts and for the comparison of them with the model calculation and satellite observations.

Finally, we discuss the effect of vertical movement of the irregularities on the GPS measurements. Its effect at the equatorial anomaly may not be significant as it may be at the magnetic equator since the irregularities observed at the anomaly is connected to those at the magnetic equator above 600-km altitude which are considered to be already in a stable state. However, plumes sometimes develop up to 1000 km, and the vertical velocity is observed to be several hundred meters per second at the growth phase of the irregularities after sunset [*Tsunoda*, 1981]. The large error bars that appeared at 1900-2100 LT in Figure 7 are considered to be due to the contribution of vertical drifts during the growth phase. Fluctuations of the zonal velocities before 2100 LT were also observed in the previous observations [*Basu et al.*, 1991]. Figure 8 explains schematically how the vertical drifts affect the correlation time. Two receivers, W and E, are spaced magnetically west-east, and the GPS satellites are seen in the western and eastern sky (GPS 1 and GPS 2, respectively). If the irregularities drift eastward without vertical drift, irregularities that passed W at t_1 may pass E at t_2. In the presence of upward movements, irregularities meet the radio waves at higher altitude at time t_2'. On the ground we measure the apparent correlation time $(t_2' - t_1)$ instead of the true correlation time $(t_2 - t_1)$, and therefore the inferred zonal velocities can be either greater or smaller than the true velocities depending on the satellite locations in the sky and depending on the drift direction of the ionospheric irregularities. Its effect will appear rather significant at early evening and during the magnetically disturbed times. In general, the GPS satellites can either be in the eastern or western sky randomly, and therefore we can remove its contribution by counting

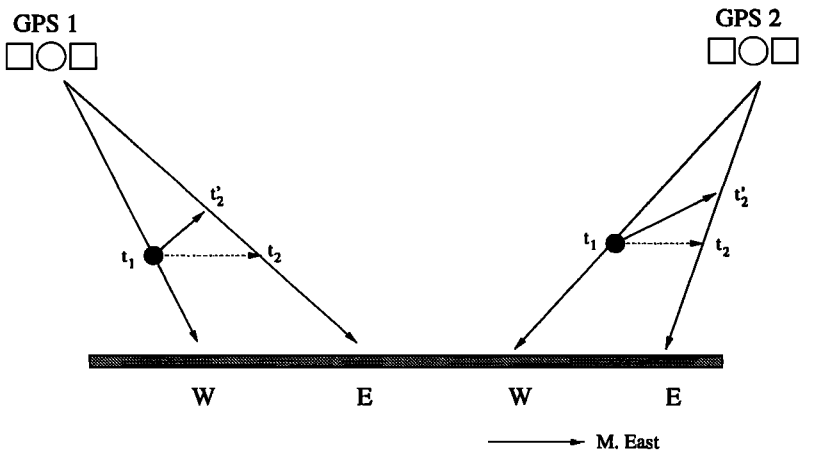

Figure 8. Schematic diagram that shows an effect of vertical drift on the correlation time.

only the measurements at high elevations and averaging them statistically using the long-term observations.

4. Summary and Future Work

The scintillation activity and ionospheric zonal apparent drifts were studied using the GPS measurements at the crest of the equatorial anomaly in Brazil. Strong scintillation activity was accompanied with large TEC depletions which were aligned along the magnetic field. Owing to an elongation of the irregularity structure along the field line the correlation length of the Fresnel scale irregularities in that direction was larger than the spaced receiver distance (70 m). The apparent eastward velocity has maximum value ranging 150-200 m/s in 2000-2100 LT, and then it decreases to $\sim$ 50-100 m/s at midnight. For a magnetically disturbed day the scintillation lasted during the whole night, and abnormal zonal plasma drifts were observed. The apparent eastward velocities on that night were smaller than those on the other nights, and their reversal occurred near midnight. Fluctuations of the apparent westward velocities were observed early in the morning, and the apparent westward velocity increased up to 100 m/s at 0500 LT.

The establishment of GPS has opened a new possibility for global study with low cost, and we could exploit it in studying radio scintillation and ionospheric zonal drift with Cornell University GPS receivers. Compared with other observations in the low-latitude region, we obtained reasonable ionospheric zonal drift velocities from the GPS measurements. In that sense, our current and future measurements of the zonal drift velocity are expected to provide a new data source in this field. Owing to the lack of ground observation data in the low-latitude region except at the magnetic equator, the zonal drift patterns at off-magnetic latitudes are not well established. Since the zonal velocities are variable with ionospheric conditions and measured values may depend on the instrumental technique, comparison of the velocities measured at different time periods using different techniques can lead to a wrong interpretation of the zonal plasma flow. For this reason, simultaneous measurements using the same technique at different latitude and longitude regions are required for a rigorous study. After the campaign, we left two receivers at Cachoeira Paulista, and data collection is being continued. We also plan to operate two GPS receivers at the magnetic equator in Brazil in the near future. Using the long-term period observations at the two places, we expect to improve the credibility of the comparison.

Acknowledgments. We thank M. A. Abdu and M. C. Kelley for their valuable discussions and T. L. Beach for his advice in preparing campaign and are also grateful to E. S. Domingos and his group at Cachoeira Paulista for the operational support. This work at Cornell was supported by the Office of Naval Research under grant N00014-92-J-1822. E. R. de Paula is grateful to FAPESP under process 1997/3342-5 and to CNPq under process 102811/98-9 for the support to the GPS project at INPE.

Janet G. Luhmann thanks Santimay Basu and another referee for their assistance in evaluating this paper.

References

Aarons, J., J. P. Mullen, J. P. Koster, R. F. daSilva, J. R. Medeiros, A. Bushby, J. Pantoja, J. Lanat, and M. R. Paulson, Seasonal and geomagnetic control of equatorial scintillations in two longitudinal sectors, *J. Atmos. Terr. Phys., 42,* 861-866, 1980.

Aarons, J., M. Mendillo, and R. Yantosca, GPS phase fluctuations in the equatorial region during the MISETA 1994 campaign, *J. Geophys. Res., 101,* 26,851-26,862, 1996.

Abdu, M. A., I. J. Kantor, I. S. Batista, and E. R. de Paula, East-west plasma bubble irregularity motion determined from spaced VHF polarimeter: Implications on velocity shear in the zonal *F* region bulk plasma motion, *Radio Sci., 20,* 111-122, 1985a.

Abdu, M. A., I. S. Batista, H. H. A. Sobral, E. R. de Paula, and I. J. Kantor, Equatorial ionospheric plasma bubble irregularity occurrence and zonal velocities under quiet and disturbed conditions from polarimeter observations, *J. Geophys. Res., 90,* 9921-9928, 1985b.

Abdu, M. A., J. H. A. Sobral, Y. Nakamura, and C. J. Zamlutti, Equatorial plasma bubble zonal velocity height gradient from spaced VHF polarimeter and scanning 630-nm measurements, *Geophys. Res. Lett., 14,* 965-968, 1987.

Aggson, T. L., N. C. Maynard, F. A. Herrero, H. G. Mayr, L. H. Brace, and M. C. Liebrecht, Geomagnetic equatorial anomaly in zonal plasma flow, *J. Geophys. Res., 92,* 311-315, 1987.

Anderson, D. N., and M. Mendillo, Ionospheric conditions affecting the evolution of equatorial plasma depletions, *Geophys. Res. Lett., 10,* 541-544, 1983.

Basu S., J. P. McClure, S. Basu, W. B. Hanson, and J. Aarons, Coordinated study of equatorial scintillation and in situ and radar observations of nighttime *F* region irregularities, *J. Geophys. Res., 85,* 5119-5130, 1980.

Basu S., S. Basu, E. Kudeki, H. P. Zengingonul, M. A. Biondi, and J. W. Meriwether, Zonal irregularity drifts and neutral winds measured near the magnetic equator in Peru, *J. Atmos. Terr. Phys., 53,* 743-755, 1991.

Basu S., et al., Scintillations, plasma drifts, and neutral winds in the equatorial ionosphere after sunset, *J. Geophys. Res., 101,* 26,795-26,809, 1996.

Batista, I. S., A. Abdu, and R. A. Medrano, Magnetic activity effects on range type spread *F* and vertical plasma drifts at Fortaleza and Huancayo as studied through ionosonde measurements and theoretical modeling, *Ann. Geophys., 8,* 357-364, 1990.

Beach, T. L., Global positioning system studies of equatorial scintillations, Ph.D. dissertation, Cornell Univ., Ithaca, N. Y., 1998.

Beach, T. L., M. C. Kelley, P. M. Kintner, and C. A. Miller, Total electron content variations due to nonclassical traveling ionospheric disturbances: Theory and Global Positioning System observations, *J. Geophys. Res., 102,* 7279-7292, 1997.

Briggs, B. H., On the analysis of moving patterns in geophysics, I, Correlation analysis, *J. Atmos. Terr. Phys., 30,* 1777-1788, 1968.

Coley, W. R., and R. A. Heelis, Low-latitude zonal and vertical ion drifts seen by DE-2, *J. Geophys. Res., 94,* 6751-6761, 1989.

Farley, D. T., E. Bonelli, B. G. Fejer, and M. F. Larsen, The prereversal enhancement of the zonal electric field in the equatorial ionosphere, *J. Geophys. Res., 91,* 13,723-13,728, 1986.

Fejer, B. G., The equatorial ionospheric electric field: A review., *J. Atmos. Terr. Phys., 43,* 377-386, 1981.

Fejer, B. G., D. T. Farley, C. A. Gonzalez, R. F. Woodman, and C. Calderon, *F* region east-west drifts at Jicamarca, *J. Geophys. Res., 86,* 215-218, 1981.

Fejer, B. G., E. R. de Paula, S. A. Gonzalez, and R. F. Woodman, Average vertical and zonal *F* region plasma drifts over Jicamarca, *J. Geophys. Res., 96,* 13,901-13,906, 1991.

Heelis, R. A., P. C. Kendall, R. J. Moffet, D. W. Windle, and H. Rishbeth, Electrical coupling of the *E* and *F* regions and its effect on *F* region drifts and winds, *Planet. Space Sci., 22,* 743-756, 1974.

Hofmann-Wellenhof, B. H. Lichtenegger, and J. Collins, *Global Positioning System: Theory and Practice,* 3rd ed., Springer-Verlag, New York, 1994.

Kelley, M. C., and T. Maruyama, A diagnostic model for equatorial spread *F*, 2, The effect of magnetic activity, *J. Geophys. Res., 97,* 1271-1277, 1992.

Kelley, M. C., D. Kotsikopoulos, T. Beach, D. Hysell, and S. Musman, Simultaneous Global Positioning System and radar observations of equatorial spread *F* at Kwajalein, *J. Geophys. Res., 101,* 2333-2341, 1996.

Kudeki, E., B. G. Fejer, D. T. Farley, and H. M. Ierkic, Interferometer studies of equatorial *F* region irregularities and drifts, *Geophys. Res. Lett., 8,* 377-380, 1981.

Maynard, N. C., T. L. Aggson, F. A. Herrero, and M. C. Liebrecht, Average low-latitude meridional electric fields from DE-2 during solar maximum, *J. Geophys. Res., 93,* 4021-4037, 1988.

Mendillo, M., and J. Baumgardner, Airglow characteristics of equatorial plasma depletions, *J. Geophys. Res., 87,* 7641-7652, 1982.

Musman, S., J. M. Jahn, J. LaBelle, and W. E. Swartz, Imaging spread *F* structures using GPS observations at Alcantara, Brazil, *Geophys. Res. Lett., 24,* 1703-1706, 1997.

Rastogi, R. G., J. P. Mullen, and E. MacKenzie, Effect of geomagnetic activity on equatorial radio VHF scintillations and spread *F*, *J. Geophys. Res., 86,* 3661-3664, 1981.

Richmond, A. D., S. Matsushita, and J. D. Tarpley, On the production mechanism of electric currents and fields in the ionosphere, *J. Geophys. Res., 81,* 547-555, 1976.

Rohrbaugh, R. P., W. B. Hanson, B. A. Tinsley, B. L. Cragin, and J. P. McClure, Images of transequatorial bubbles based on field-aligned airglow observations from Haleakala in 1984-1986, *J. Geophys. Res., 94,* 6736-6770, 1989.

Sobral, J. H. A., and M. A. Abdu, Latitudinal gradient in the plasma bubble zonal velocities as observed by scanning 630-nm airglow measurements, *J. Geophys. Res., 95,* 8253-8257, 1990.

Sobral, J. H. A., and M. A. Abdu, Solar activity effects on equatorial plasma bubble zonal velocity and its latitude gradient as measured by airglow scanning photometers, *J. Atmos. Terr. Phys., 53,* 729-742, 1991.

Spatz, D. E., S. J. Franke, and K. C. Yeh, Analysis and interpretation of spaced receiver scintillation data recorded at an equatorial station, *Radio Sci., 23,* 347-361, 1988.

Tinsley, B. A., R. P. Rohrbaugh, W. B. Hanson, and A. L. Broadffot, Images of transequatorial *F* region bubbles in 630- and 777-nm emissions compared with satellite measurements, *J. Geophys. Res., 102,* 3057-3077, 1997.

Tsunoda, R. T., Time evolution and dynamics of equatorial backscatter plumes, 1, Growth phase, *J. Geophys. Res, 86,* 139-149, 1981.

Vacchione, J. D., S. J. Franke, and K. C. Yeh, A new analysis technique for estimating zonal irregularity drifts and variability in the equatorial *F* region using spaced receiver scintillation data, *Radio Sci., 22,* 745-756, 1987.

Valladares, C. E., R. Sheehan, S. Basu, H. Kuenzler, and J. Espinoza, The multi-instrumented studies of equatorial thermosphere aeronomy scintillation system: Climatology of zonal drifts, *J. Geophys. Res, 101,* 26,839-26,850, 1996.

Wernik, A. W., C. H. Liu, and K. C. Yeh, Modeling of spaced-receiver scintillation measurements, *Radio Sci., 18,* 743-764, 1983.

Woodman, R. F., East-west ionospheric drifts at the magnetic equator, *Space Res., 12,* 969-974, 1972.

Woodman, R. F., and C. La Hoz, Radar observations of *F* region equatorial irregularities, *J. Geophys. Res, 81,* 5447-5466, 1976.

Zalesak, S. T., S. L. Ossakow, and P. K. Chaturvedi, Nonlinear equatorial spread *F*: The effect of neutral winds and background Pedersen conductivity, *J. Geophys. Res, 87,* 151-166, 1982.

H. Kil and P. M. Kintner, School of Electrical Engineering, 304 Rhodes Hall, Cornell University, Ithaca, NY 14853. (hkil@ee.cornell.edu; paul@ee.cornell.edu)

E. R. de Paula and I. J. Kantor, C. P. 515, INPE-DAE, 12.201-970 São José dos Campos, São Paulo, Brazil. (eurico@dae.inpe.br; kantor@dae.inpe.br)

(Received July 6, 1999; revised November 24, 1999; accepted November 24, 1999.)